International Journal of Solids and Structures 46 (2009) 3313–3320

Contents lists available at ScienceDirect

International Journal of Solids and Structures

journal homepage: www.elsevier.com/locate/ijsolstr

Adaptive sensing of kinematic entities in the vicinity of a time-dependent geometrically nonlinear pre-deformed state ☆

Michael Krommer, Yury Vetyukov *,[1]

Institute for Technical Mechanics, Johannes Kepler University Linz, Altenbergerstrasse 69, 4040 Linz, Austria

ARTICLE INFO

Article history:
Received 17 December 2008
Received in revised form 22 April 2009
Available online 6 May 2009

Keywords:
Continuously distributed strain-type sensors
Geometric nonlinearity
Adaptive sensing
Nonlinear rod theory

ABSTRACT

A continuously distributed strain-type sensor can be designed to produce a signal proportional to a desired kinematic entity in the geometrically linear range. The corresponding spatial distribution of the sensor is found as a solution to an auxiliary problem of statics. For a geometrically nonlinear setting we suggest a new general method to design continuous strain-type sensors for measurements in the vicinity of a known pre-deformed state. This method is formulated for a general three-dimensional continuum, and a numerical implementation for rod structures is presented. The efficiency is first demonstrated for a nonlinear static deformation of a spatial rod structure; the modern approach to numerical modeling of rods with no shear deformation is utilized. Another example of in-plane vibrations of a rod demonstrates the benefit of the adaptive recomputation of the sensor distribution accounting for the actual time-dependent pre-deformation.

1. Introduction

Smart structure technology has become a key technology in the design of modern, so-called intelligent, civil, mechanical and aerospace structures. Similar to human beings, these intelligent or smart systems are capable to react to disturbances exerted upon them by the environment they are operating in. For reviews, see Crawley (1994), Tani et al. (1998) and for future challenges and opportunities, see Liu et al. (2005a). Practical applications of smart structures are, e.g. in the fields of active structural vibration control (Alkhatib and Golnaraghi, 2003) as well as active noise control (Gopinathan et al., 2001; Irschik et al., 2003).

The design of the smart structure is a highly multi-disciplinary task, which involves the modeling of the structure, the interrogation and communication of the structure with a controller by means of suitable sensing and actuation, the integration of the smart system in the structure and the implementation of the system. One key aspect for a successful design is the communication between structure and controller, the so-called control–structure interaction (Gabbert and Tzou, 2001). Sensors and actuators are responsible for the functioning of this communication. Sensors provide information about the state the structure is in; this information has to be interpreted and properly processed by the controller to provide the actuator with information about what to do. For a discussion of strategic issues in the sensor design, see Liu et al. (2005b), and for frontiers in sensors/sensor systems, see Glaser et al. (2005). In typical continuous systems a crucial point is the spatial distribution of sensors to obtain proper information as well as to perform distributed control of continua (Gabbert and Tzou, 2001). Finding these distributions for geometrically nonlinear problems is the main topic of the present paper.

In particular, we consider continuously distributed (or simply continuous) strain-type sensors. Those produce a signal that represents a weighted integral over the strain a body is suffering, in contrast to discrete strain-type sensors, whose signal is a sum of local strain values. In the geometrically linear regime continuous sensors are well studied: e.g. Lee and Moon (1990) introduced the concept of shaping the electrode pattern of a piezoelectric layer to measure a specific modal amplitude of a vibrating plate; the latter sensors are denoted as modal sensors. With respect to the application of modal sensors a vast amount of literature exists; we mention only Tzou and Hollkamp (1994) and Sun and Tong (2001). Besides using continuous strain-type sensors as modal sensors other types have been reported in the literature; e.g. nilpotent sensors (Miu, 1992; Irschik et al., 1999a) or displacement sensors (Irschik et al., 1999b).

A detailed discussion on the possible use of continuous strain-type sensors to measure a large variety of different structural entities was presented by Krommer and Irschik (2007); however, the

☆ Part of this work has been presented at the 4th European Conference on Structural Control, September 2008, St. Petersburg, Russia (see Vetyukov and Krommer, 2008).

* Corresponding author. Tel./fax: +43 732 2468 9793.
E-mail addresses: michael.krommer@jku.at (M. Krommer), yury.vetyukov@jku.at (Yu. Vetyukov).
[1] On leave from the Department of Computer Technologies in Engineering, St. Petersburg State Polytechnical University, Polytechnicheskaya ul. 29, 195251 St. Petersburg, Russia.

0020-7683/$ - see front matter © 2009 Elsevier Ltd. All rights reserved.
doi:10.1016/j.ijsolstr.2009.04.024

method for the design of continuous strain-type sensors in Krommer and Irschik (2007) was restricted to linear problems only. In the present paper we extend this method to the geometrically nonlinear regime. Although there is a large amount of literature available discussing structural problems with embedded strain-type sensors and actuators in the geometrically nonlinear regime (Tylikowski and Frischmuth, 2003; Cheng et al., 2005), no effort has yet been undertaken to study the effect of geometrical nonlinearities upon the design of strain-type sensors, rather than the effect on the sensor signal of a pre-designed sensor itself. In the present paper, we present a first account for the design of continuous strain-type sensors in a geometrically nonlinear regime; in particular, we seek, in extension to the linear case, to measure structural entities of a small motion superposed upon a finite pre-deformation.

In Section 2 the proposed sensor design is discussed within a fully three-dimensional setting. In Section 2.1 the linear case for measuring a particular kinematic entity is summarized. It is shown that the distribution of the sensor coincides with a static stress distribution in an auxiliary problem with an applied force loading, to which the particular kinematic entity to be measured is the work conjugate. In Section 2.2 we introduce the sensor signal for the geometrically nonlinear problem as a spatially weighted integral over the Green–Lagrangian strain tensor; based on this definition of a continuous strain-type sensor, we study sensing in the vicinity of a pre-deformed configuration in Section 2.3. It turns out that the sensor distribution can again be computed from an auxiliary static problem; yet, forces have to be applied in the pre-deformed configuration resulting into a static Cauchy stress distribution, which depends on the pre-deformation. The sensor distribution is then found by transforming this static stress distribution to the undeformed configuration. In Section 3 the method is applied to nonlinear rod structures. We present results for the sensor design in the vicinity of a statically pre-deformed spatial rod configuration first, and then proceed with dynamic problems. In the latter dynamic case we also discuss the design of adaptive sensors, for which the distribution is changed in time in order to account for time-dependent rod configurations.

2. Continuous strain-type sensors: three-dimensional formulation

2.1. The geometrically linear case

We consider a three-dimensional solid body with the field of infinitesimal displacements $\boldsymbol{u}(\boldsymbol{r})$; $\boldsymbol{r}$ is the position vector of a material point in the undeformed configuration. Let V be the undeformed volume of the body, $\boldsymbol{r} \in V$. The strain tensor is $\boldsymbol{\varepsilon} = \nabla \boldsymbol{u}^S$, and the stress tensor is denoted as $\boldsymbol{\tau}$; ∇ is the invariant differential operator, and a superscript S stands for the symmetric part of a tensor.

The local signal of a continuous strain-type sensor within the body is proportional to the components of the local strain: $\boldsymbol{\tau}_s \cdot\cdot\, \boldsymbol{\varepsilon}$; the components of the tensor $\boldsymbol{\tau}_s$ are weights assigned to each component of the strain tensor. The overall signal Y of a continuously distributed sensor is the integral over the local sensors, and depends on the strain field within the material body:

$$Y[\boldsymbol{\varepsilon}(\boldsymbol{r})] = \int_V \boldsymbol{\tau}_s(\boldsymbol{r}) \cdot\cdot\, \boldsymbol{\varepsilon}(\boldsymbol{r}) dV = \int_V \boldsymbol{\tau}_s(\boldsymbol{r}) \cdot\cdot \nabla \boldsymbol{u}(\boldsymbol{r})^S dV. \tag{1}$$

The volume of the body is supposed to be identical to the volume of the sensor, i.e. the strain value is assumed to be available for each point of the body.

A comprehensive study on the design of such strain-type sensors in the geometrically linear case has been presented by Krommer and Irschik (2007). Here we just review the solution for one specific problem; suppose we are interested in measuring $u_*[\boldsymbol{u}(\boldsymbol{r})] = \boldsymbol{e} \cdot \boldsymbol{u}(\boldsymbol{r}_*)$ – the displacement of the point $\boldsymbol{r}_*$ in the direction $\boldsymbol{e}$. The weights of the continuous sensor $\boldsymbol{\tau}_s(\boldsymbol{r})$ should be chosen such that the equality

$$Y[\nabla \boldsymbol{u}^S] = u_*[\boldsymbol{u}] \tag{2}$$

holds for any kinematically admissible $\boldsymbol{u}$.

To find the spatial weights, an auxiliary problem with a fictitious static loading, the work conjugate of which is the measured entity, is solved. We consider the body V with a set of homogeneous kinematic boundary conditions, which do not allow for a rigid body motion. The kinematic boundary conditions must be chosen such that the original displacement field $\boldsymbol{u}(\boldsymbol{r})$ is kinematically admissible for the auxiliary problem. A unit force $\boldsymbol{f} = 1\boldsymbol{e}$ is applied in the point $\boldsymbol{r}_*$ such that its work on a displacement field $\boldsymbol{u}$ equals the measured entity $\boldsymbol{e} \cdot \boldsymbol{u}(\boldsymbol{r}_*)$; there is no traction force applied at the boundary ∂V. For the auxiliary problem we compute a statically admissible stress field $\boldsymbol{\tau}_f$; then $\boldsymbol{\tau}_s(\boldsymbol{r}) \equiv \boldsymbol{\tau}_f$.

To prove that this choice for $\boldsymbol{\tau}_s$ results in (2) we apply the virtual work principle (see e.g. Eliseev, 1999; Malvern, 1969). In the position of static equilibrium:

$$\int_V (\boldsymbol{f} \cdot \delta \boldsymbol{u} + \delta A^{(i)}) dV = 0, \quad \delta A^{(i)} = -\boldsymbol{\tau}_f \cdot\cdot \nabla \delta \boldsymbol{u}^S \tag{3}$$

for any kinematically admissible $\delta \boldsymbol{u}(\boldsymbol{r})$. Here, the assumption on geometric linearity is important: the expression of the virtual work of the internal forces $\delta A^{(i)}$ in general would include the differential operator in the deformed configuration, which is identical to ∇ only in the linear case.

Substituting the actual displacements field $\boldsymbol{u}$ instead of $\delta \boldsymbol{u}$ in (3), we prove the equality of the signal to the kinematic entity we are seeking to measure:

$$Y[\boldsymbol{\varepsilon}] = \int_V \boldsymbol{\tau}_s \cdot\cdot\, \boldsymbol{\varepsilon}\, dV = \int_V \boldsymbol{\tau}_f \cdot\cdot \nabla \boldsymbol{u}^S dV = \int_V \boldsymbol{f} \cdot \boldsymbol{u}\, dV = u_*. \tag{4}$$

This chain of reasoning with the principle of virtual work remains valid for a broad class of continuous structures: rods, shells, etc. The loading $\boldsymbol{f}$ in the auxiliary problem must have as a work conjugate the measured kinematic entity in terms of virtual work (see Krommer and Irschik, 2007). Instead of one field $\boldsymbol{\tau}_s = \boldsymbol{\tau}_f$ several sensing functions according to the force factors can appear (e.g. in-plane stresses and bending moments for shells). Possible singularities in the solution of the auxiliary problem with a concentrated force can be avoided, if the measured displacement is averaged over some small part of the body, resulting in a problem with distributed forces. Kinematic entities on the boundary can be measured as well, by accounting for additional static tractions applied in the auxiliary problem.

2.2. Continuous strain-type sensors in a geometrically nonlinear setting

As long as the deformations are small, the sensor signal is determined by (1). The extension of this formula to finite deformations requires the concepts of the nonlinear geometry of deformation. Consider a material body with the position vector $\boldsymbol{r}$ of the points in the reference configuration, which occupies the volume $\overset{\circ}{V}$; the corresponding differential operator is $\overset{\circ}{\nabla}$. In this usually undeformed configuration the sensors produce no signal. In some pre-deformed configuration with the volume V the new position vector is

$$\boldsymbol{R} = \boldsymbol{R}(\boldsymbol{r}), \quad \mathbf{F} = \overset{\circ}{\nabla} \boldsymbol{R}^T, \quad \nabla = \mathbf{F}^{-T} \cdot \overset{\circ}{\nabla}, \quad \mathbf{E} = \frac{1}{2}(\mathbf{F}^T \cdot \mathbf{F} - \mathbf{I}). \tag{5}$$

The deformation gradient tensor $\mathbf{F}$ relates the differential operator in the pre-deformed configuration ∇ to the original one $\overset{\circ}{\nabla}$, $\mathbf{E}$ is the Green–Lagrangian strain tensor, and $\mathbf{I}$ is the identity tensor.

For practical computations one needs to deal with the components of the tensorial quantities. If a set of three material coordinates q^i is chosen such that $\boldsymbol{r} = \boldsymbol{r}(q^i)$, then three basis vectors can be introduced as $\boldsymbol{r}_i = \partial \boldsymbol{r}/\partial q^i$. In the deformed configuration the corresponding basis vectors are $\boldsymbol{R}_i$. The covariant components of the strain tensor are

$$E_{ij} = \boldsymbol{r}_i \cdot \mathbf{E} \cdot \boldsymbol{r}_j = \frac{1}{2}(\boldsymbol{R}_i \cdot \boldsymbol{R}_j - \boldsymbol{r}_i \cdot \boldsymbol{r}_j), \tag{6}$$

Those components are known to be related to the extensions of the material fibers and the angle changes between them (Lurie, 2005); the expression in brackets is equal to the change of the components of the metric tensor from the undeformed to the deformed configuration. The effect of choosing other Lagrangian strain tensors (e.g. Biot or logarithmic) would be of higher order of smallness and therefore insignificant for engineering structures, where local stretches are always small in a normal working regime – whereas large overall deformations and rotations are not excluded. In analogy to the linear case, the signal of a continuous strain-type sensor is assumed to be proportional to the extensions and angle changes in each point. It is reasonable to assume that we are measuring

$$Y[\mathbf{E}(\boldsymbol{r})] = \int_{\mathring{V}} S_s^{ji}(\boldsymbol{r}) E_{ij}(\boldsymbol{r}) d\mathring{V} = \int_{\mathring{V}} \mathbf{S}_s(\boldsymbol{r}) \cdot\cdot \mathbf{E}(\boldsymbol{r}) d\mathring{V}, \tag{7}$$

summation over the repeated indices is implied. The contravariant components S_s^{ji} are the weights assigned to the corresponding local strains, and the tensor field $\mathbf{S}_s(\boldsymbol{r}) = S_s^{ji}\boldsymbol{r}_j\boldsymbol{r}_i$ does not directly depend on the deformation. In the geometrically linear case this is equivalent to (1).

An alternative energy related interpretation of a strain-type sensor in geometrically nonlinear problems would be as follows. Together with the actual structure we consider the continuous sensor as a fictitious background body with some pre-stress $\mathbf{S}_s(\boldsymbol{r})$:

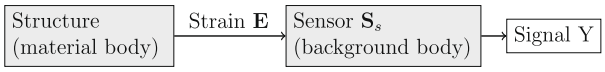

The background body deforms together with the structure and has the same strain $\mathbf{E}$; in contrast, we assume the background body not to affect the material body, because we do not consider actuation in the present work. If the pre-stress $\mathbf{S}_s$ is understood as a second Piola–Kirchhoff stress tensor, then the virtual work of the sensor per unit volume in the undeformed configuration is $\delta A^{(S)} = -\mathbf{S}_s \cdot\cdot \delta\mathbf{E}$. Hence, the signal of the continuous sensor Y equals the potential energy of the background body. Moreover, if the pre-stress $\mathbf{S}_s$ is constant in time, then we once again arrive at (7). This interpretation appears to be convenient for the extension of using strain-type sensors for active control of flexible structures in the geometrically nonlinear regime, as modern trends in control theory are closely related to the flow of energy between structure, sensors, actuators and controller; see e.g. Kugi (2001) and Ortega et al. (2001).

2.3. Sensor design in the vicinity of a pre-deformed state

For finite deformations a sensor with a given distribution $\mathbf{S}_s(\boldsymbol{r})$ cannot produce a signal, which is proportional to a given kinematic entity. Consider, e.g. pure bending of a clamped beam with a moment at the free end. The curvature of the beam changes with the moment linearly, and so do the local strain components in the fibers of the beam; hence, the measured signal will always remain proportional to the loading. However, the vertical tip displacement depends on the moment even non-monotonously; e.g. it turns back to zero as the beam is bent into a circle. A possible solution is to develop sensors, which are designed for measurements in the vicinity of a known pre-deformed state.

Consider a small additional deformation; the actual position vector is $\boldsymbol{R}_u = \boldsymbol{R} + \boldsymbol{u}$. The pre-deformed configuration $\boldsymbol{R}(\boldsymbol{r})$ is known, and some component of the displacement $\boldsymbol{u}$ is to be measured. The new value of the signal (7) corresponds to the new strain tensor $\mathbf{E}_u$, linearized with respect to $\boldsymbol{u}$ (Eliseev, 1999; Bonet and Wood, 1997):

$$Y_u = Y[\mathbf{E}_u], \quad \mathbf{E}_u = \mathbf{E} + \mathbf{F}^T \cdot \boldsymbol{\varepsilon} \cdot \mathbf{F}, \quad \boldsymbol{\varepsilon} = \nabla \boldsymbol{u}^S, \tag{8}$$

in which the small strain tensor $\boldsymbol{\varepsilon}$ relative to the pre-deformed configuration appears. Transforming the expression of Y_u and introducing the volumetric coefficient $J = \det \mathbf{F}$, we arrive at an integral over the deformed volume:

$$Y_u - Y = \int_V \boldsymbol{\tau}_s \cdot\cdot \boldsymbol{\varepsilon}\, dV, \quad \boldsymbol{\tau}_s = J^{-1}\mathbf{F} \cdot \mathbf{S}_s \cdot \mathbf{F}^T. \tag{9}$$

The left-hand side here is a signal relative to the known signal level $Y[\mathbf{E}]$ in the pre-deformed configuration; the form of the integral is identical to (1). Therefore, the modified sensing functions $\boldsymbol{\tau}_s$ can be determined applying the procedure, presented in Section 2.1, to the known pre-deformed shape of the body. The field of stresses $\boldsymbol{\tau}_s$ should balance the loading $\boldsymbol{f}$ in the auxiliary problem:

$$\nabla \cdot \boldsymbol{\tau}_s + \boldsymbol{f} = \mathbf{0}. \tag{10}$$

The work conjugate of the loading $\boldsymbol{f}$ is again the measured kinematic entity u_* – the displacement relative to the pre-deformed configuration. Integrating the inner product of (10) with a field of displacements $\boldsymbol{u}$ over the volume we arrive at

$$\int_V (\nabla \cdot \boldsymbol{\tau}_s \cdot \boldsymbol{u} + \boldsymbol{f} \cdot \boldsymbol{u}) dV = 0, \quad \int_V \boldsymbol{f} \cdot \boldsymbol{u}\, dV = u_*[\boldsymbol{u}]. \tag{11}$$

The transformation to (9) follows with the Gauss theorem on divergence:

$$\begin{aligned} u_* &= -\int_V \nabla \cdot \boldsymbol{\tau}_s \cdot \boldsymbol{u}\, dV = \int_V (-\nabla \cdot (\boldsymbol{\tau}_s \cdot \boldsymbol{u}) + \boldsymbol{\tau}_s \cdot\cdot \nabla \boldsymbol{u}^T) dV \\ &= -\int_{\partial V} \boldsymbol{n} \cdot \boldsymbol{\tau}_s \cdot \boldsymbol{u}\, dS + \int_V \boldsymbol{\tau}_s \cdot\cdot \boldsymbol{\varepsilon}\, dV = Y_u - Y. \end{aligned} \tag{12}$$

The integral over the boundary ∂V is zero:

$$\partial V = \partial V_1 \cup \partial V_2, \quad \boldsymbol{u} = \mathbf{0} \text{ at } \partial V_1, \quad \boldsymbol{n} \cdot \boldsymbol{\tau}_s = \mathbf{0} \text{ at } \partial V_2 \tag{13}$$

there is no traction force on the free surface in the auxiliary problem.

The distribution of the sensor weights in the undeformed configuration follows from (9):

$$\mathbf{S}_s = J\mathbf{F}^{-1} \cdot \boldsymbol{\tau}_s \cdot \mathbf{F}^{-T}, \tag{14}$$

which is identical to the transformation between the Cauchy stress tensor and the second Piola–Kirchhoff stress tensor.

Another more formal way to the same result would be to directly consider the variation of the signal (7) for the sensing function $\mathbf{S}_s$ satisfying the balance conditions (10) and (13) through (14). After the transformations we conclude that

$$\delta Y = \int_V \boldsymbol{f} \cdot \delta \boldsymbol{R}\, dV \quad \text{with } \mathring{\nabla} \cdot (\mathbf{S}_s \cdot \mathbf{F}^T) + J\boldsymbol{f} = \mathbf{0}. \tag{15}$$

The three main steps for the sensor design are:

Step 1. The pre-deformed configuration $\boldsymbol{R}(\boldsymbol{r})$ is determined as a solution of a geometrically nonlinear problem.
Step 2. The auxiliary problem of statics for this pre-deformed configuration is solved in a linear setting, producing $\boldsymbol{\tau}_s$.
Step 3. The actual sensing functions for the undeformed configuration $\mathbf{S}_s$ are computed from (14).

The presented mathematical manipulations were carried out in the invariant form. If the geometrically nonlinear problem for predeformation and the linear auxiliary problem are solved with the same set of material coordinates q^i (practically speaking, the same

finite element discretization is applied twice), then the practical computation can be implemented in a rather straightforward manner. The components of the strain tensor (6) are additive functions with respect to deformation: the variations $\delta E_{ij} = (\boldsymbol{R}_i \cdot \delta \boldsymbol{R}_j)^S$ do not contain information on the metrics $\boldsymbol{r}_i \cdot \boldsymbol{r}_j$ in the undeformed state. Therefore, the relation between the components of the solution of the auxiliary problem τ_s and the actual sensing functions S^{ij} is simple:

$$\delta Y = \int_V \tau_s^{ji} \delta E_{ij}\, dV = \int_{\mathring{V}} S_s^{ji} \delta E_{ij}\, d\mathring{V} \;\Rightarrow\; S_s^{ji} = J\tau_s^{ji}, \tag{16}$$

the same could be deduced from (14). Provided that the appropriate coordinates are chosen, the third step of the algorithm consists of simple multiplication of the components of the Cauchy stress tensor, obtained as a solution to the auxiliary problem, with the volumetric coefficient J.

The practical application of this technique to real three-dimensional bodies is doubtful due to the following reasons:

- massive three-dimensional constructions do seldom display significant geometrically nonlinear behavior in normal working regimes;
- implementing a continuous sensor capable of measuring all components of the strain tensor is a nontrivial task.

However, this is not the case for thin-walled structures, such as rods or shells.

3. Sensing in rod structures

3.1. Nonlinear theory of rods with no shear

Our approach for sensing in the vicinity of a pre-deformed configuration can be easily applied to rods: the corresponding strain measures are additive quantities, and the sensing functions for the auxiliary problem need not be recomputed to the undeformed configuration. In this Section the basic ideas of the theory of rods as material lines (Antman, 1972; Eliseev, 1999) are presented.

We consider a one-dimensional Cosserat continuum: each particle is a rigid body with six degrees of freedom. The position vector of the particles $\boldsymbol{r}(s)$ is a function of the Lagrangian coordinate s. Three basis vectors $\boldsymbol{e}_i(s)$ are associated with each particle to specify its orientation. In the undeformed configuration we have $\boldsymbol{r}_0(s)$ and $\boldsymbol{e}_{i0}(s)$, and here s is the arc coordinate: $\boldsymbol{r}_0' \cdot \boldsymbol{r}_0' = 1$. The curvature and twist of the rod are defined by the vector $\boldsymbol{\Omega}$:

$$\boldsymbol{e}_k' = \boldsymbol{\Omega} \times \boldsymbol{e}_k, \quad \boldsymbol{\Omega} = \frac{1}{2}\boldsymbol{e}_k \times \boldsymbol{e}_k' = \Omega_k \boldsymbol{e}_k. \tag{17}$$

The rotation tensor $\mathbf{P}$ and the deformation vector $\boldsymbol{\kappa}$ are introduced:

$$\mathbf{P} = \boldsymbol{e}_k \boldsymbol{e}_{0k}, \quad \mathbf{P}' = \boldsymbol{\kappa} \times \mathbf{P}, \quad \boldsymbol{\kappa} = \boldsymbol{\Omega} - \mathbf{P} \cdot \boldsymbol{\Omega}_0. \tag{18}$$

The components of the vector $\boldsymbol{\kappa} = \kappa_k \boldsymbol{e}_k$ are equal to the change of the components of the twist and curvature vector $\boldsymbol{\Omega}$ due to deformation: $\kappa_k = \Omega_k - \Omega_{0k}$; the components Ω_k and Ω_{0k} are considered in the deformed $\boldsymbol{e}_k$ and undeformed $\boldsymbol{e}_{0k}$ bases, respectively. As it was noted at the beginning of this Section, the strain measures κ_k are additive with respect to deformation.

For thin rods the classical model of Kirchhoff with no extension and no shear effects is often applicable. However, efficient numerical modeling demands the extension of the rod to be unconstrained. Therefore, a model with extension, but constrained shear is advantageous. In this model the tangent vector to the rod axis $\boldsymbol{r}'(s)$ rotates together with the corresponding particle:

$$\boldsymbol{r}'(s) = (1+\varepsilon)\mathbf{P} \cdot \boldsymbol{e}_{30} = (1+\varepsilon)\boldsymbol{e}_3, \tag{19}$$

the third direction is now tangent to the axis, $\boldsymbol{e}_{30} = \boldsymbol{r}_0'(s)$; ε is the deformation of extension, κ_3 is the deformation of twist, and κ_α – of bending ($\alpha = 1, 2$).

The particle with the coordinate $s + 0$ acts on the neighbouring particle $s - 0$ with the moment $\boldsymbol{M}(s)$ and the force $\boldsymbol{Q}(s)$. The principle of virtual work for the one-dimensional continuum of particles with six degrees of freedom leads to the known equations of balance of the force factors (Antman, 1972; Eliseev, 1999)

$$\boldsymbol{Q}' + \boldsymbol{q} = \boldsymbol{0}, \quad \boldsymbol{M}' + \boldsymbol{r} \times \boldsymbol{Q} + \boldsymbol{m} = \boldsymbol{0}, \tag{20}$$

$\boldsymbol{q}$ and $\boldsymbol{m}$ being the external forces and moments acting on the particles. The elastic relations are written in terms of the function of the strain energy per unit length

$$\Pi_1 = \Pi_1(\kappa_k, \varepsilon), \quad \boldsymbol{M} = \frac{\partial \Pi_1}{\partial \kappa_k}\boldsymbol{e}_k, \quad Q_3 = \frac{\partial \Pi_1}{\partial \varepsilon}. \tag{21}$$

The transversal shear force $\boldsymbol{Q}_\perp = Q_\alpha \boldsymbol{e}_\alpha$ is determined from the constraint Eq. (19). In the simplest case the strain energy is a quadratic form with no coupling,

$$\Pi_1 = \frac{1}{2}a_{ij}\kappa_i\kappa_j + \frac{1}{2}b\varepsilon^2, \quad \boldsymbol{M} = \mathbf{a} \cdot \boldsymbol{\kappa} = a_{ij}\kappa_i \boldsymbol{e}_j, \quad Q_3 = b\varepsilon. \tag{22}$$

The stiffnesses a_{ij} can be taken from the linear model of the rod. The deformation of extension is often of no actual interest, and the term $\frac{1}{2}b\varepsilon^2$ in the strain energy can be considered as a penalty function.

3.2. Sensor design for spatial deformations of rod structures

In this section we are seeking to design continuous sensors, which are capable of measuring kinematic entities in the course of spatial deformations of rods. The following assumptions apply:

- the rod is equipped with sensors with arbitrary distribution;
- three strain values are available in each cross-section, which can be recomputed to κ_i by means of a linear transformation;
- the deformation of extension ε is negligible.

Then the sensor signal is

$$Y[\kappa_i] = \int_0^L M_{si}\kappa_i\, ds = \int_0^L M_{si}(\Omega_i - \Omega_{0i})ds. \tag{23}$$

The choice of the three sensing functions $M_{si}(s)$ includes two steps: first, the nonlinear problem is solved and the pre-deformed state is determined; second, the linear auxiliary problem in the vicinity of the pre-deformed state is solved. According to the discussion of Eq. (16), there is no need to recompute the sensing functions to the undeformed state in this case: the same material coordinate $q^1 \equiv s$ is used all the time, and there is no difference between integration over the deformed and the undeformed configurations, as the deformation of extension ε is negligible.

Instead of the volumetric formulation, discussed in Section 2, in (23) we deal with an integral over the one-dimensional continuum. However, the presented above conclusions for the linear analysis are based on the principle of virtual work, which is certainly applicable for rod structures. Validity of the analysis in the vicinity of a pre-deformed state, discussed in Section 2.3 for general three-dimensional bodies, can also be proven mathematically with the equations of the classical theory of inextensible rods.

The approach is easier to explain by applying it to a sample problem. The considered rod structure is presented in Fig. 1. A quarter of a circular rod is clamped and bent with an out-of-plane tip force F; the length of the rod is $L = \pi/2$, and the cross-section is a circle with the radius 0.01; for the sake of readability the International System of Units (SI) is understood in the following.

In the position of static equilibrium the total energy of the system Π is minimal,

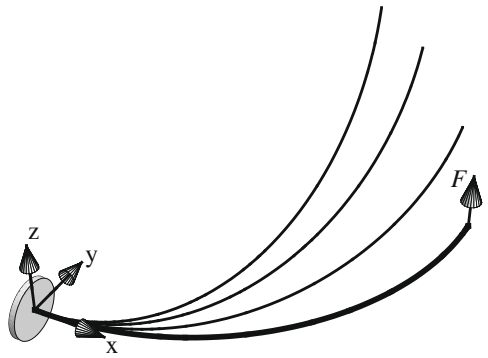

Fig. 1. Spatial bending: curved rod (thick) and deformed states (thin).

$$\Pi = \Pi^{(def)} + \Pi^{(ext)} = \min, \quad \Pi^{(def)} = \int_0^L \Pi_1 \, ds, \quad \Pi^{(ext)} = -Fr_z(L). \tag{24}$$

Numerical minimization is usually performed by means of the Ritz method: we approximate the rod axis $\boldsymbol{r}(s)$ and the orientation of particles $\boldsymbol{e}_i(s)$ as a combination of N shape functions with the coefficients q_k, $k = 1, \ldots, N$. A special technique is used such that the constraint (19) holds for any q: the particles can rotate only around the axis of the rod (Eliseev and Vetyukov, 2008). The strain measures κ_i and ε are then functions of q and s. We integrate (22) over the length of the rod and compute the total energy Π as a function of the generalized coordinates. Then the equilibrium path can be determined from computing the minimum of $\Pi(q)$ for each value of F.

The computations were performed by using the commercially available software package Mathematica.[2] A global Ritz approximation of the shape of the rod is chosen for this sample problem instead of full-scale finite element modeling to reduce the computational effort. Several computed equilibrium positions are shown in Fig. 1 as thin lines.

We consider some certain force value F_0 and the corresponding actual equilibrium configuration q_0. Suppose that we are interested in measuring the x and z coordinates of the tip, when the configuration of the rod is near q_0. To design the sensors the linear auxiliary problem must be solved. For $q = q_0 + \hat{q}$ with $\hat{q}$ being a small deviation, we linearize the original strain measures

$$\kappa_i = \kappa_{i0} + \hat{\kappa}_i + \cdots, \quad \varepsilon = \varepsilon_0 + \hat{\varepsilon} + \cdots, \tag{25}$$

$\hat{\kappa}_i$ and $\hat{\varepsilon}$ are linear with respect to $\hat{q}$. In order to formulate the linear auxiliary problem we consider now the actual configuration q_0 as undeformed. The new deformations take place relative to this configuration, and the quadratic strain energy is $2\widehat{\Pi}_1 = a_{ij}\hat{\kappa}_i\hat{\kappa}_j + b\hat{\varepsilon}^2$. Although s is not exactly the arc coordinate in the actual configuration q_0, this effect is negligible since ε_0 is small. Integrating $\widehat{\Pi}_1$ over the length, we get a quadratic form of the strain energy $\widehat{\Pi}^{(def)}$. It would have been incorrect simply to extract the quadratic terms from (24): the dependence of the strain measures κ_i on the generalized coordinates q is nonlinear, and the stiffness of the original system near the pre-deformed state differs from the stiffness in the auxiliary problem.

To measure the tip displacement in the x direction we solve the auxiliary problem with the unit force acting on the tip in the x direction. In the numerical procedure we minimize the quadratic function,

$$\hat{q}^{(x)} = \arg\min(\widehat{\Pi}^{(def)} - \hat{x}(L)). \tag{26}$$

[2] Wolfram Research, http://www.wolfram.com.

With the solution of this linear problem we compute the sensing functions as the moments, which correspond to the unit loading, the work conjugate of which is the measured displacement:

$$M_{si}^{(x)}(s) = M_i = a_{ij}\hat{\kappa}_j|_{\hat{q}=\hat{q}^{(x)}}. \tag{27}$$

Analogously we compute the sensing functions $M_{si}^{(z)}(s)$, which measure the z displacement of the tip. The corresponding signals $Y^{(x)}$ and $Y^{(z)}$ (23) are recomputed to the measured tip coordinates as

$$x_* = x_0 + Y^{(x)} - Y_0^{(x)}, \quad z_* = z_0 + Y^{(z)} - Y_0^{(z)}. \tag{28}$$

Here x_0, z_0 and $Y_0^{(x,z)}$ are the tip coordinates and the signals in the pre-deformed state; hence, we estimate the displacement as the increment of the signal $Y - Y_0$.

3.3. Numerical results for spatial rod deformation

The sensors are tested on the exact solution of the sample problem: the actual tip coordinates $x(L)$ and $z(L)$ on the equilibrium path with varying F (thicker lines in Fig. 2) are compared with the values x_* and z_*, which are measured for the corresponding solution. Two sensor designs were applied:

- in the vicinity of the undeformed state (fully linear formulation) in order to estimate the influence of the geometric nonlinearity on the measurement error – dashed thin lines,
- in the vicinity of the pre-deformed state with the force F_0 (according to the approach presented above) – solid thin lines.

One can see that the x coordinate is measured incorrectly with the linear sensor: the x displacement appears as a pure geometrically nonlinear effect; using the sensor designed for the pre-deformed state improves the situation. For the z coordinate the situation is less dramatic, but one can see that the linear sensor and the one for the pre-deformed configuration have different domains of applicability.

The numerical modeling of the sample problem and the design of the sensors were accomplished by virtue of the same Ritz approximation with $N = 20$ shape functions and unknown coefficients. In practical applications we can expect that the accuracy of the solution of the auxiliary problem plays an important role on the overall precision of measurements. On the contrary, for the solution of the nonlinear problem of pre-deformation it is sufficient to remain in the vicinity of the actual state. Therefore, for the broad class of statically determinate problems a simplified approach can be suggested. The pre-deformed configuration is found with some approximate method, and the distribution of moments in the solution of the auxiliary problem can be computed simply from the equilibrium conditions (20). This strategy will be utilized in the following dynamical example. However, for complicated statically indeterminate structures the presented procedure of derivation of the quadratic strain energy $\widehat{\Pi}$ for the auxiliary problem is necessary. Finite element discretization can be more efficient than the global Ritz approximation used in the presented sample problem.

3.4. Finite in-plane oscillations of a cantilever

Dynamical modeling of rod structures is especially simple for in-plane problems: the configuration of a rod with no shear is fully determined by the planar curve of its axis. Another simplification is that there is only one sensing function $M_s(s)$ in this case, which corresponds to the single component of the bending moment.

We consider bending of a cantilever beam with a time-varying tip force, Fig. 3. The length of the beam is $L = 1$, the radius of the circular cross-section is 0.005, and the material properties

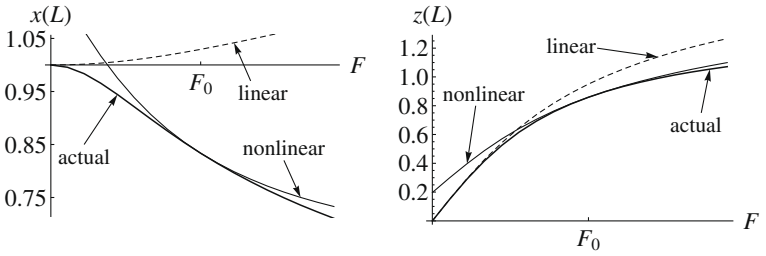

Fig. 2. Measured and actual tip coordinates for the equilibrium path.

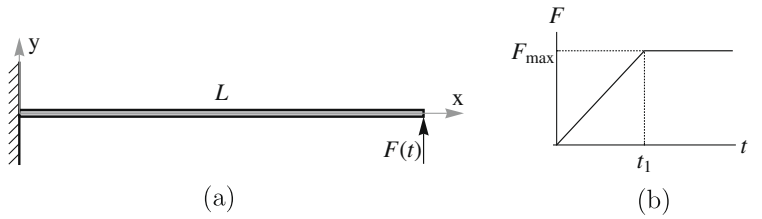

Fig. 3. Plane bending: cantilever (a) and time-varying force (b).

correspond to steel. The force increases linearly during the time interval $0 \leqslant t \leqslant t_1 = 0.1$ and then remains at the constant level $F_{max} = 200$.

Rod finite elements were implemented in Mathematica with independent third-order approximation of the functions $x(s)$ and $y(s)$ over the element: nodal degrees of freedom are then the positions $\boldsymbol{r}(s)$ and the derivatives $\boldsymbol{r}'(s)$, which guarantees smoothness of the axis of the rod. The simulation results are obtained from a model with four finite elements (overall 20 degrees of freedom, 3 of which are constrained due to clamping at the left end).

The modeled dynamical behavior of the rod is presented in Fig. 4. Both, the x and y coordinates of the tip display oscillatory behavior in time (solid line) near the quasistatic solution, which corresponds to the current value of the force $F(t)$ (dashed line). The static deflection due to the force F_{max}, computed with the simple formula of the linear beam theory, is shown with the dotted line above the plot of the y coordinate to show the effect of the geometric nonlinearity.

3.5. Adaptive sensing in dynamics

Suppose that we know the loading history and the corresponding quasistatic solution for each time instance. Our goal is to develop a sensor which would measure the deformation of the beam during the dynamical process. Three different sensor designs can be applied:

- based on the fully linear formulation (initial state sensor);
- based on the quasistatic solution for $F = F_{max}$ (final state sensor);
- based on the quasistatic solution for the actual force value $F(t)$ (adaptive sensor).

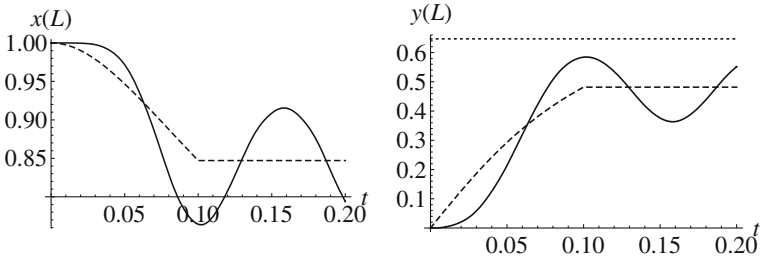

Fig. 4. Tip coordinates in dynamic (solid) and quasistatic (dashed) solutions.

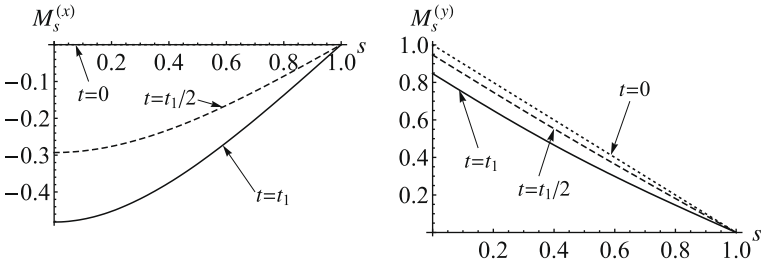

Fig. 5. Evolution of the sensing functions.

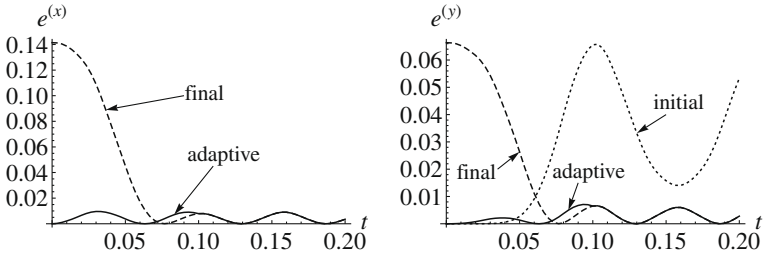

Fig. 6. Measurement errors of the tip coordinates for the three sensor designs.

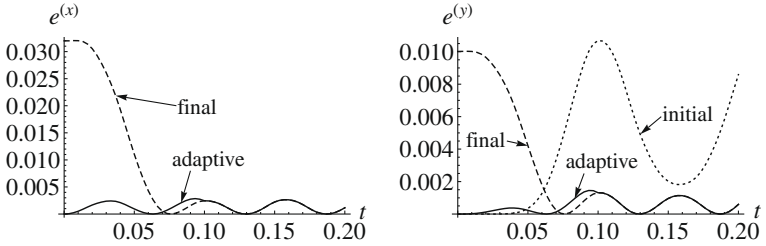

Fig. 7. Measurement errors of the coordinates of the middle of the beam.

The measured estimations of the coordinates of the tip are again computed from (28), whereas the reference values x_0, y_0 depend on the chosen reference pre-deformed configuration. Each of the two signals is defined by its own single sensing function:

$$Y^{(x)}[\kappa] = \int_0^L M_s^{(x)} \kappa \, ds, \quad Y^{(y)}[\kappa] = \int_0^L M_s^{(y)} \kappa \, ds, \tag{29}$$

the curvature κ can easily be computed for known $x(s)$ and $y(s)$.

As it was mentioned previously, in this statically determinate problem the sensing functions can be found from the balance equations. If the reference solution of the quasistatic problem is $x_r(s), y_r(s)$ (initial configuration, final or intermediate for the adaptive sensor), then we just have to compute the moments resulting from unit forces $f_x = 1$ or $f_y = 1$ at the tip of the rod:

$$M_s^{(x)}(s) = f_x(-y_r(L) + y_r(s)), \quad M_s^{(y)}(s) = f_y(x_r(L) - x_r(s)). \tag{30}$$

In Fig. 5 the evolution of the sensing functions is shown with three reference quasistatic configurations varying in time; $M_s^{(x)}$ is identical to zero for the initial configuration.

Applying the developed sensors to the computed dynamical behavior of the rod, we can plot the measurement errors $e^{(x)} = x_* - x(L)$ and $e^{(y)} = y_* - y(L)$ as functions of time, see Fig. 6. Two errors are plotted for $e^{(x)}$: the initial state sensor does not work in this case. The final state sensor becomes identical to the adaptive one at $t > t_1$, which shows the best overall behavior.

With the same procedure sensors for the measurement of the coordinates of the middle point of the beam were developed; sensing functions are then equal to zero as $s > L/2$. Resulting errors of measurement with the three designs of the sensor are plotted in Fig. 7.

4. Conclusions

A new approach for the design of continuously distributed strain-type sensors for the measurement of kinematic entities in structures undergoing finite deformations is discussed in the paper. The actual state is supposed to remain in the vicinity of a known reference pre-deformed configuration. In the case of constant or slowly varying large forces, acting on the system, this pre-deformed configuration can be the solution of a nonlinear problem of statics, and the distribution of the sensors can be dynamically updated in time to achieve the best behavior.

The presented method can be used to study the kinematical characteristics of the deformation of a structure. In combination with the use of so-called nilpotent sensors (Miu, 1992; Irschik et al., 1999a), which produce a zero signal as long as the deformation of the structure remains in the linear range and no kinematical constraints are violated, the method can be applied for the purpose of health monitoring: appearance of local buckling or plastic zones in the structure can be detected. Analyzing the signal of several nilpotent sensors, one can even conclude on the region of the structure, in which the defect is developing.

Some possible issues were not addressed in the text of the present paper and may be studied in the future.

- The recomputation of surface strains in the material of the cross-section to the rod strain measures is a nontrivial task: relations between κ_i and the three-dimensional deformed state can be obtained with a reliable rod theory, which results from the asymptotic analysis of a three-dimensional problem of elasticity (see Yeliseyev and Orlov, 1999). Moreover, the distribution of sensors within the cross-section should also be optimized in the framework of such an analysis.
- The deformation of extension is supposed to be fully negligible both for the kinematics of the rod as well as for the sensor signal. However, together with shear deformations it can also affect the functioning of the strain-type sensors. This influence should be estimated.
- While the idealized formulation with continuously distributed sensors may work perfectly, discrete sensor distributions lead to different results. Placement of sensors over the length of the beam and their weights may be optimized according to many different criteria. For a linear setting the problem was already studied in Krommer et al. (2009); an analysis of the nonlinear formulation is yet missing.
- Changing the sensing function in time has some contradiction with the argumentation for the formula (7), which is connected to the potential energy of the background body. Indeed, for

piezoelectric sensors some additional procedures are needed to correctly obtain the signal of a sensor with a distribution depending on time.

The presented method may also be applied to other structures; e.g. shell structures undergoing finite deformations. Yet, modern formulations of the theory of shells and efficient simulation strategies must be utilized.

The results of the present research can be used in combination with feed-back methods for the control of finite deformations. For the problem of damping vibrations the developed sensors can produce the feed-back signal for the controller, which then would provide the input signal for distributed actuators. Nonetheless, it remains to study the proper design of the latter actuators for geometrically nonlinear problems in some future work.

Acknowledgements

Support of the authors from the Austrian Science Fund (FWF Translational Project L441-N41 "Sensor Systems for Structural and Health Monitoring") and of M. Krommer from the Austrian Center of Competence in Mechatronics (ACCM) is gratefully acknowledged.

References

Alkhatib, R., Golnaraghi, M.F., 2003. Active structural vibration control: a review. Shock and Vibration Digest 35 (5), 367–383.

Antman, S.S., 1972. The theory of rods. Handbuch der Physik, vol. VI a/2. Springer, Berlin, pp. 641–703.

Bonet, J., Wood, R.D., 1997. Nonlinear Continuum Mechanics for Finite Element Analysis. Cambridge University Press, Cambridge, MA.

Cheng, J., Wang, B., Du, S.Y., 2005. A theoretical analysis of piezoelectric/composite anisotropic laminate with larger-amplitude deflection effect, Part I: Fundamental equations. International Journal of Solids and Structures 42 (24-25), 6166–6180.

Crawley, E.F., 1994. Intelligent structures for aerospace: a technology overview and assessment. AIAA Journal 32 (8), 1689–1699.

Eliseev, V.V., 1999. Mechanics of Elastic Bodies (in Russian). State Polytechnical University Publishing House, St. Petersburg.

Eliseev, V., Vetyukov, Yu., 2008. Modeling of spatial rod systems with geometrical and physical nonlinearity. In: Proceedings of Seventh International Conference on Reliability of Materials and Structures, St. Petersburg, Russia, June 2008.

Gabbert, U., Tzou, H.S., 2001. Preface: Proceedings of IUTAM-Symposium on Smart Structures and Structronic Systems, Magdeburg, Germany, September 2000.

Glaser, S.D., Shoureshi, R.A., Pescovitz, D., 2005. Frontiers in sensors and sensing systems. Smart Structures and Systems 1 (1), 103–120.

Gopinathan, S.V., Varadan, V.V., Varadan, V.K., 2001. Active noise control studies using the Rayleigh–Ritz method. In: Proceedings of IUTAM-Symposium on Smart Structures and Structronic Systems, Magdeburg, Germany, September 2000.

Irschik, H., Krommer, M., Belyaev, A.K., Schlacher, K., 1999a. Shaping of piezoelectric sensors/actuators for vibrations of slender beams: coupled theory and inappropriate shape functions. Journal of Intelligent Material Systems and Structures 9, 546–554.

Irschik, H., Krommer, M., Pichler, U., 1999b. Shaping of distributed piezoelectric sensors for flexural vibrations of smart beams. In: Proceedings of SPIE's 6th Annual International Symposium on Smart Structures and Materials, Newport Beach, CA, March 1999.

Irschik, H., Krommer, M., Nader, M., Pichler, U., 2003. Dynamic piezoelectric shape control applied of shells of revolution with translatory support excitation. In: Proceedings of US & Europe Workshop on Sensors and Smart Structures Technology, Como, Italy, April 2002.

Krommer, M., Irschik, H., 2007. Sensor and actuator design for displacement control of continuous systems. Smart Structures and Systems 3 (2), 147–172.

Krommer, M., Zellhofer, M., Heilbrunner, K.-H., 2009. Strain-type sensor networks for structural monitoring of beam-type structures. Journal of Intelligent Material Systems and Structures (in press), doi:10.1177/1045389x08099467.

Kugi, A., 2001. Non-linear Control Based on Physical Models. Springer, London.

Lee, C.-K., Moon, F.-C., 1990. Modal sensors/actuators. Journal of Applied Mechanics 57, 434–441.

Liu, S.-C., Tomizuka, M., Ulsoy, G., 2005a. Challenges and opportunities in the engineering of intelligent structures. Smart Structures and Systems 1 (1), 1–12.

Liu, S.-C., Tomizuka, M., Ulsoy, G., 2005b. Strategic issues in sensors and smart structures. In: Proceedings of Third European Conference on Structural Control, Vienna, Austria, July 2004.

Lurie, A.I., 2005. Theory of Elasticity. Springer, Berlin.

Malvern, L.E., 1969. Introduction to the Mechanics of a Continuous Medium. Prentice-Hall, Englewood Cliffs, NJ.

Miu, D.K., 1992. Mechatronics: Electromechanics and Contromechanics. Springer, New York.

Ortega, R., van der Schaft, A.J., Mareels, I., Maschke, B., 2001. Putting energy back to control. Control Systems Magazine 21, 18–33.

Sun, D., Tong, L., 2001. Modal control of smart shells by optimized discretely distributed piezoelectric transducers. International Journal of Solids and Structures 38 (18), 3281–3299.

Tani, J., Takagi, T., Qiu, J., 1998. Intelligent material systems: application of functional materials. Applied Mechanics Review 51, 505–521.

Tylikowski, A., Frischmuth, K., 2003. Stability and stabilization of circular plate parametric vibrations. International Journal of Solids and Structures 40 (19), 5187–5196.

Tzou, H.S., Hollkamp, JJ., 1994. Collocated independent modal control with self-sensing orthogonal piezoelectric actuators (theory and experiment). Smart Materials and Structures 3, 277–284.

Vetyukov, Yu., Krommer, M., 2008. Optimal sensing of kinematic quantities in the vicinity of a pre-deformed state in a geometrically nonlinear setting. In: Proceedings of Fourth European Conference on Structural Control, St. Petersburg, Russia, September 2008.

Yeliseyev, V.V., Orlov, S.G., 1999. Asymptotic splitting in the three-dimensional problem of linear elasticity for elongated bodies with a structure. Journal of Applied Mathematics and Mechanics 63 (1), 85–92.